



Research Article

Novel Ultrahard C₆ with Mixed sp³-sp² Hybridizations and Semiconducting Behavior: Crystal Chemistry and First Principles Investigations

Samir F. Matar

CMMS, Lebanese German University (LGU), Jounieh P.O. Box 206, Lebanon
E-mail: s.matar@lgu.edu.lb

Received: 6 December 2022; **Revised:** 1 January 2023; **Accepted:** 29 January 2023

Abstract: Novel tetragonal carbon allotrope C₆ made of allene-like C(sp²) tricarbon unit >C=C=C< embedded in diamond-like C(sp³) lattice is proposed from crystal chemistry backed with first principles (DFT) pointing to localized charge density around tetrahedral C(sp³) and smeared charge along linear allene-like tricarbon unit characteristic of C(sp²) hybridization. From phonons band structures C₆ is dynamically stable characterized with particularly high optical phonon frequency $\omega = 60$ THz assigned to antisymmetric C-C-C stretching mode, also identified as I.R. active in isolated C₃H₄ allene molecule. Novel C₆ is found mechanically stable with large Vickers hardness. The electronic band structure reveals semi-conducting electronic properties. Hybrid electronic configurations C(sp³)-C(sp²) identified in *nanodiamonds* benefit from a growing interest in different fields of materials science, whence the relevance of novel C₆ allotrope as model for such investigations.

Keywords: carbon; hybrids, semi-conductors; hard materials; phonons; hardness; DFT

1. Introduction

Identifying novel carbon allotropes is an active research field targeting materials with specific characteristics such as mechanical properties approaching diamond by using modern materials research software based on evolutionary crystallography [1]. The known carbon allotropes are assembled in SACADA database thus helping researchers avoiding claims of structurally related systems as novel allotropes [2]. Novel allotropes proposed are curated, recorded, and published with the Cambridge Structural Database (CSD) (cf. ref. [3] for presently studied carbon allotrope C₆).

Another initial search protocol lies in crystal chemistry underlying structural “engineering”. We recently proposed body-centered tetragonal bct-C₄ (Figure 1a) in space group $I\bar{4}m2$ as template for other original carbon allotropes close to diamond. As a matter of fact bct-C₄ exhibits alternative representation of cubic diamond upon considering primitive cells [4]. The removal of the body center carbon as schematized with the red arrow in Fig. 1a leads to a simple tetragonal structure with eight tetrahedra occupying the corner positions (Fig. 1b). The space group symmetry is lowered and becomes identified as $P\bar{4}m2$. The resulting C₃ then serves as template structure for filling the empty space left by central carbon removal. Beside bct-C₄ recovered with one tetrahedral sp³, i.e., C(tet.), two, and three carbon interstitials enter as trigonal (sp²) C(trig.) atoms modifying the tetrahedral diamond-like structure significantly while bringing new structure - properties relationships. Such investigations constitute the aim of this paper through the study of the electronic, mechanical, and dynamic properties of novel carbon

Copyright ©2023 Samir F. Matar

DOI: <https://doi.org/10.37256/ujcr.1120232219>

This is an open-access article distributed under a CC BY license
(Creative Commons Attribution 4.0 International License)

<https://creativecommons.org/licenses/by/4.0/>

allotrope with mixed $C(sp^3) / C(sp^2)$ hybridizations: C_6 . In fact, there is a large interest in systems containing such mixed hybridizations such as in the B-C-O system [5].

The structural investigations need to be further analyzed with quantum mechanical calculations to derive quantities describing accurately the targeted function, such as hardness and electronic band structure, together with the dynamic stability, etc. Most accurate framework is the Density Functional Theory (DFT) [6,7] used herein with DFT-built computations.

The insertion of two trigonal carbons leading to tet- C_5 (Fig. 1c) was recently studied [8] with the outcome of stable ultrahard carbon allotrope with metallic behavior. Herein, we examine the effect of inserting three carbon atoms into C_3 giving C_6 stoichiometry. Then, C_6 is made of 3 $C(tet.)$ and 3 $C(trig.)$ as schematized in Fig. 1d with colored spheres, i.e., red, and yellow for the two types of $C(trig.)$ –cf. Table 1.

With respect to C_5 shown with two trigonal carbons depicted with yellow spheres, an additional trigonal carbon is introduced at the cell center (red sphere). The novel structure shows the particularity of linear $C=C=C$ connecting the two layers of tetrahedra along c - vertical direction. The “ $>C=C<$ ” configuration resembles “allene” or *propadiene* molecule when hydrogen atoms are attached to terminal carbons in the isolated molecule (Fig. 1e).

Note that linear tricarbon motifs exist in the rhombohedral structure of refractory abrasive $B_{12}C_3$ [9], and in tricarbon molecule that was proposed in the solid state in two cohesive structures from DFT investigations [10].

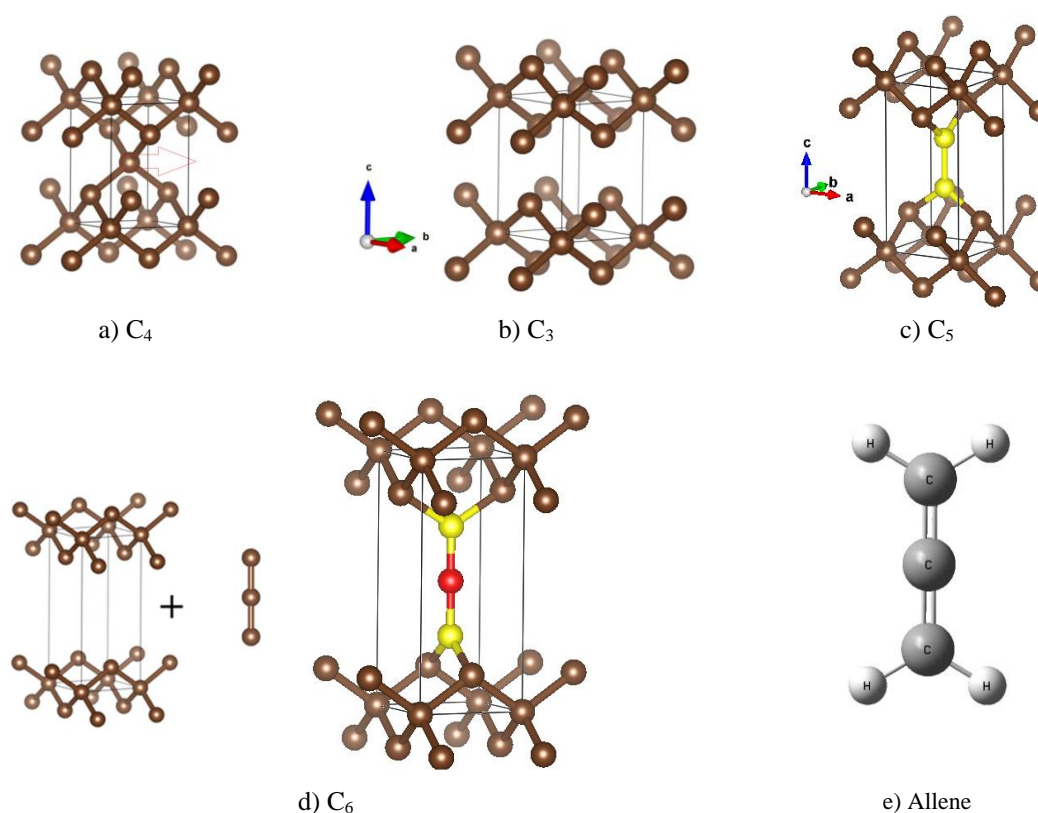


Figure 1. Sketches of the crystal structures, a) C_4 , b) C_3 , c) C_5 , and d) C_6 with schematics of transformation from C_3 ; yellow and red spheres indicating the trigonal carbons; e) C_3H_4 allene (propadiene) molecule.

Table 1. Crystal structure parameters of tetragonal C₃, C₅ [8], and C₆. Lattice constants and distances are in units of Å (Volume in Å³). Energies are in eV

$P\bar{4}m2$, N°115	C ₃	C ₅ [8]	C ₆
<i>a</i>	2.521	2.4786	2.624
<i>c</i>	3.402	5.0279	6.029
C1(tet.)	(1 <i>a</i>) 0, 0, 0	(1 <i>a</i>) 0, 0, 0	(1 <i>a</i>) 0, 0, 0
C2(tet.)	(2 <i>g</i>) ½, 0, <i>z</i> <i>z</i> = 0.237	(2 <i>g</i>) ½, 0, <i>z</i> <i>z</i> = 0.187	(2 <i>g</i>) ½, 0, <i>z</i> <i>z</i> = 0.149
C1(trig.)	-	-	(1 <i>c</i>) ½, ½, ½
C2(trig.)	-	(2 <i>f</i>) ½, ½, <i>z</i> <i>z</i> = 0.646	(2 <i>f</i>) ½, ½, <i>z</i> <i>z</i> =0.285
Volume (Å ³)	21.63	30.89	41.52
<i>d</i> _{C1(tet.)-C2(tet.)}	1.50	1.55	1.59
<i>d</i> _{C2(tet.)-C2(trig.)}	-	1.50	1.55
<i>d</i> _{C1(trig.)-C2(trig.)}	-	-	1.30
<i>d</i> _{C2(trig.)-C2(trig.)}	-	1.46	-
<i>E</i> _{total}	-21.58	-43.26	-51.16
<i>E</i> _{coh/at.}	-0.59	-2.05	-1.93

2. Computational methodology

The search for the ground state structures with minimal energies was carried out with unconstrained geometry optimizations with DFT-based plane-wave Vienna Ab initio Simulation Package (VASP) package [11,12] using projector augmented wave (PAW) method for potentials [12,13], and treating the DFT exchange-correlation (XC) effects using a generalized gradient approximation (GGA) [14]. A conjugate-gradient algorithm was used in this computational scheme to relax the atoms onto the ground state. The tetrahedron method with Blöchl *et al.* corrections [15] and Methfessel-Paxton scheme [16] was applied for both geometry relaxation and total energy calculations. Brillouin-zone integrals were approximated using **k**-point sampling of Monkhorst and Pack [17]. The optimization of the structural parameters was performed until the forces on the atoms were less than 0.02 eV/Å, and all stress components below 0.003 eV/Å³. The plane wave energy cut-off was 500 eV. The protocol followed is to start from a small mesh of **k** points and to increase precision in successive calculations until the energy and the lattice constants do not change anymore thus providing the configuration with minimal energy recognized as the ground state. The investigation of the mechanical properties was based on the calculations of the elastic properties determined by performing finite distortions of the lattice and deriving the elastic constants from the strain-stress relationship. The calculated elastic constants C_{ij} are then used to obtain the bulk (B) and the shear (G) moduli with Voigt's [18] averaging method based on a uniform strain. Besides the mechanical properties the dynamic stability is determined from the phonons described as quanta of vibrations. They are illustrated with phonon band structures obtained using "Phonopy" interface code based on Python language [19]. The structure representations were obtained thanks to VESTA graphical program [20]. For assessing the electronic properties, the band structures were obtained with the all-electrons augmented spherical wave method ASW [21].

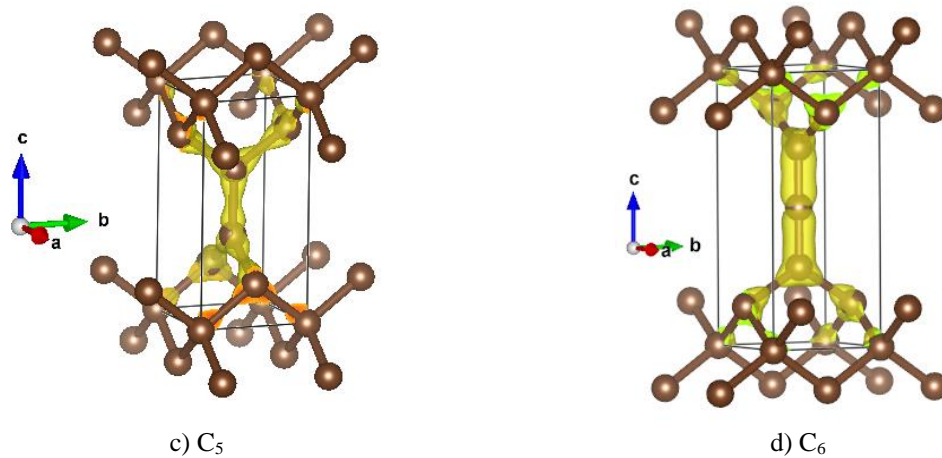


Figure 2. Charge density projections (yellow volumes)

3.2 Mechanical properties

The calculated sets of elastic constants C_{ij} are given in Table 2, reporting the values formerly obtained for C_5 [8] for the sake of comparison. Diamond-like C_4 's C_{ij} are largest while smallest magnitudes are obtained for C_3 whose structure is produced by removing the central carbon of C_4 , as shown in Fig. 1a & b. In both C_5 and C_6 the largest C_{ij} magnitude is observed for C_{33} pertaining to the rigidity along the c-axis with trigonal carbons.

All C_{ij} ($i=j$ and $i \neq j$) values are positive and their combinations obey rules pertaining to the mechanical stability: C_{ii} ($i=1, 3, 4, 6$) > 0 ; $C_{11} > C_{12}$, $C_{11} + C_{33} - 2C_{13} > 0$; and $2C_{11} + C_{33} + 2C_{12} + 4C_{13} > 0$. The equations providing the bulk B_V and shear G_V moduli are as follows for the tetragonal system [22]:

$$B_{Voigt}^{tetr.} = 1/9 (2C_{11} + C_{33} + 2C_{12} + 4C_{13}); G_{Voigt}^{tetr.} = 1/15 (2C_{11} + C_{12} + 2C_{33} - 2C_{13} + 6C_{44} + 3C_{66})$$

The corresponding B_V and G_V magnitudes are shown at the last columns of Table 2 found for C_5 and C_6 with larger values for the former, while C_3 has the smallest bulk and shear moduli. Both C_5 and C_6 show magnitudes smaller than diamond: $B_V = 445$ GPa, and $G_V = 530$ GPa [23].

Furthering on the analysis of the zero-pressure bulk modulus B_0 , the energy-volume, $E(V)$, equation-of-state (EOS) was calculated around minima found from geometry optimization.

The resulting values are plotted in Fig. 3. The $E = f(V)$ curve shows a quadratic behavior. The fit with 3rd order Birch-Murnaghan EOS [24]

$$E(V) = E_0(V_0) + [9/8]V_0B_0[(V_0/V)^{2/3} - 1]^2 + [9/16]B_0(B' - 4)V_0[(V_0/V)^{2/3} - 1]^3$$

provides E_0 , V_0 , B_0 , and B' , respectively. The equilibrium energy, volume, bulk modulus, and its pressure derivative B' are given in the insert.

The fit parameters reproduce the magnitudes of the values in Table 1 for the energy and the volume and B_0 is close to the value obtained from Voigt B_V (Table 2).

The EOS results provide further support to the calculational protocol hitherto followed.

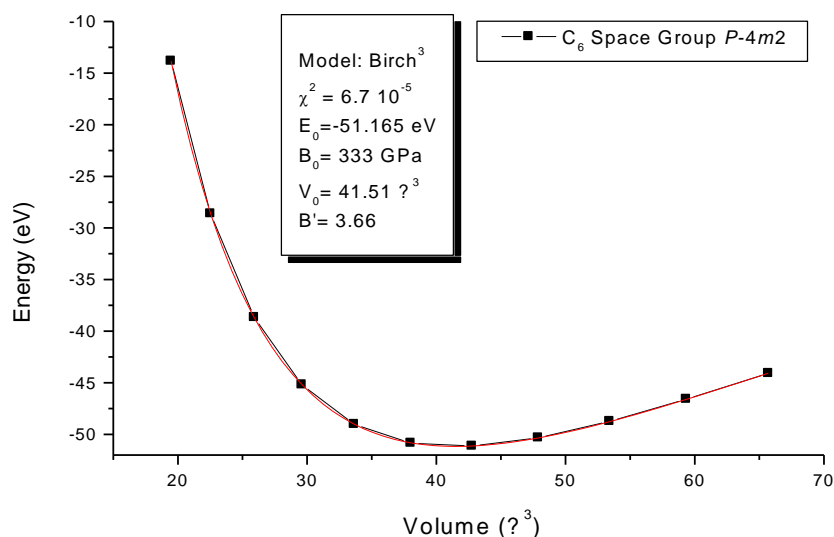


Figure 3. tet.C₆: Energy-volume curve and Birch 3rd order EOS (see text) fit with equilibrium values in the insert

Vickers hardness (H_V) was subsequently predicted using Lyakhov-Oganov (LO) approach [25] considering the topology of the crystal structure, the strength of covalent bonding, the degree of ionicity, and directionality on one hand, and the Mazhnik-Oganov (MO) [26] model using the elastic properties on the other hand. The calculated magnitudes are shown in the last columns of Table 2. The values of diamond are also provided at the end of Table 2 [23].

Expectedly diamond has the largest hardness with close values with the two models. Despite different magnitudes obtained for C₃, C₅, and C₆ due to the different approaches of the two models, it is found that C₅ and C₆ have close and high hardness values, ~20 GPa lower than diamond; letting consider them both as ultra-hard allotropes due to the aligned C-C and C-C-C along the c-axis. Oppositely C₃ has very small hardness magnitudes and it can be considered as soft.

Table 2. Calculated elastic constants and bulk B_V and shear G_V moduli in GPa units

	C ₃	C ₅ [8]	C ₆
C ₁₁	696	918	728
C ₁₂	20	10	20
C ₁₃	33	122	85
C ₃₃	155	1169	1161
C ₄₄	10	197	160
C ₆₆	5		70
B_V	191	390	330
G_V	115	414	341
H_{Vick}^{LO}	26	81	78
H_{Vick}^{MO}	19	76	74

Diamond [23]: $H_{Vick}^{LO}=90$; $H_{Vick}^{MO}=100$ GPa

3.3 Dynamic properties from the phonons

Another criterion of stability is obtained from the phonons. The energy $E = \hbar\omega$ is quantized through the Planck constant 'h' used in its reduced form \hbar ($\hbar = h/2\pi$) and multiplied by the frequency ω . Besides C_3 the phonon band structure of C_5 [7] and presently studied C_6 are shown in Fig. 3. Within VASP code, the force constants are obtained from finite displacements within the ground state structure file (8 in tet. C_6), then we proceed to summing up the forces of the different configurations leading to the dynamical matrix. The phonon frequencies are the obtained and plotted along the different directions of the Brillouin zone. Along the horizontal direction, the bands are along the main lines of the tetragonal Brillouin zone BZ (reciprocal k- space). Along the vertical direction the frequencies are given in units of terahertz (THz). Since no negative frequency magnitudes are observed in all three panels, the structures are considered as dynamically stable. There are $3N-3$ optical modes at higher energy than three acoustic modes starting from zero energy ($\omega = 0$) at the Γ point (BZ center), up to a few Terahertz. The 3 acoustic modes correspond to the lattice rigid translation modes of the crystal (two transverse and one longitudinal). The remaining bands correspond to the optic modes, culminating at $\omega \sim 40$ THz in C_5 , a magnitude observed for diamond by Raman spectroscopy [23], and only up to 34 in less stable C_3 (cf. Table 1). C_6 exhibits similar phonon spectrum as C_3 especially for the optical mode at ~ 35 THz. The two higher magnitude bands correspond to the C-C-C stretching: at $\omega \sim 40$ THz for symmetric stretching and at highest frequency magnitude of $\omega \sim 60$ THz for antisymmetric stretching.

Further check of these observations was carried out with quantum molecular structure calculations of C_3H_4 allene molecule (cf. Fig. 1d) within DFT. Focusing on the stretching modes, only the antisymmetric stretching mode was observed in C_3H_4 I.R. spectrum at $\nu=1931\text{ cm}^{-1}$ as shown in Fig. 3d featuring the most intensive line; such mode is inactive in Raman. With $1\text{ THz} = 33.356\text{ cm}^{-1}$, we calculate the corresponding value in THz: $\nu = 58\text{ THz}$, close to $\omega = 60\text{ THz}$ in crystalline solid C_6 . The results showing close magnitudes between the free molecule and the embedded $>C=C<$ on one hand and the isolation of the phonon lines at $\omega \sim 40$ and at $\omega \sim 60\text{ THz}$ on the other hand, further validate the assignment of "allene-like" label to tricarbon unit as embedded in a tetrahedral $C(\text{sp}^3)$ structure.

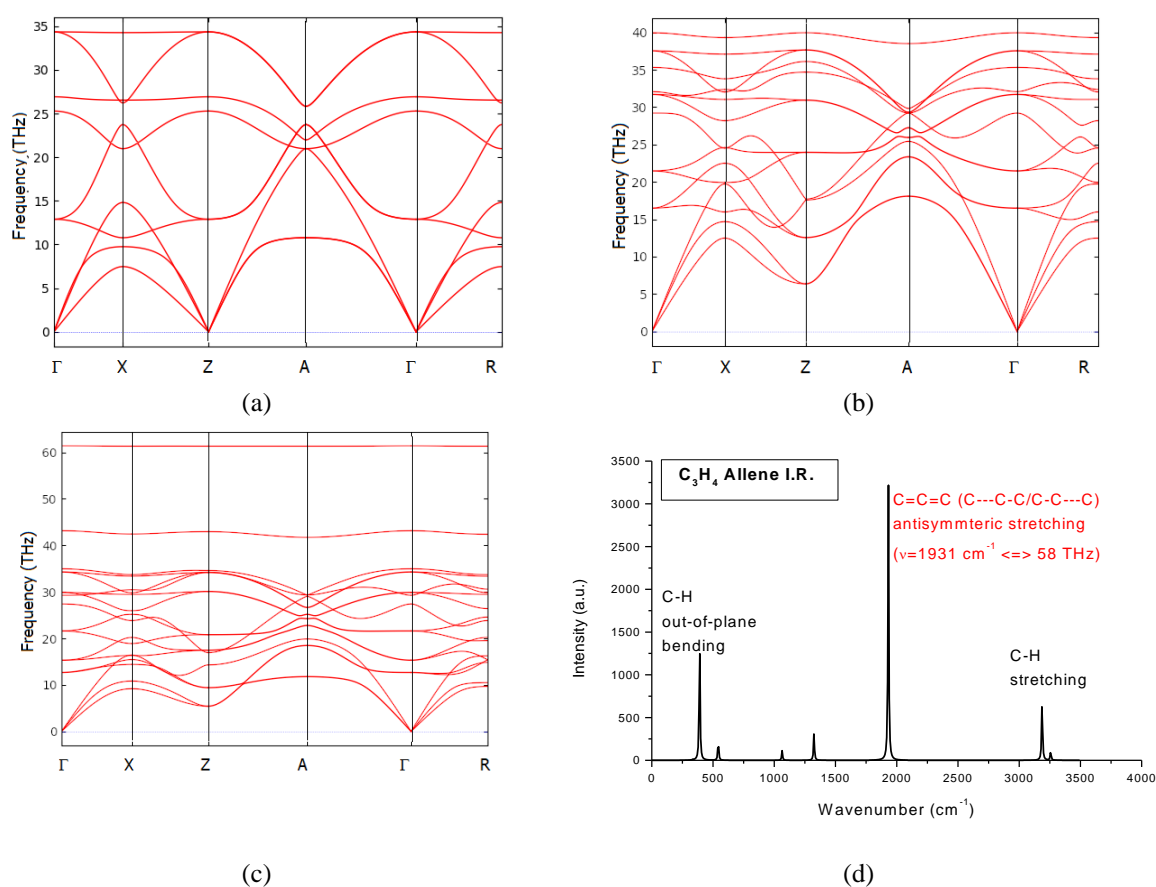


Figure 4. Phonons band structures of a) C_3 , b) C_5 , and c) C_6 . d) Calculated I.R. spectrum of allene molecule C_3H_4 with assignment of major lines

The thermodynamic properties such as entropy S and heat capacity at constant volume C_v were then calculated from the phonon frequencies using statistical thermodynamics [28]. Fig. 4 shows the change with temperature of the calculated entropy and heat capacity of tet- C_6 in comparison with corresponding experimental data for diamond [29]. Expectedly, entropy S increases with temperature. Heat capacity C_v increases and follows a nonlinear evolution tending to a flattening at highest temperature. The experimental values of diamond follow similar trend but remain below the C_6 C_v curve, except at the highest temperatures where the diamond experimental point becomes close to the C_6 green curve. It can be suggested that the difference arises from the electronic structure difference between the two carbon allotropes, i.e., insulating for diamond and semi-conductor for C_6 as shown below. Thermal conductivity details are provided in a recent work [30].

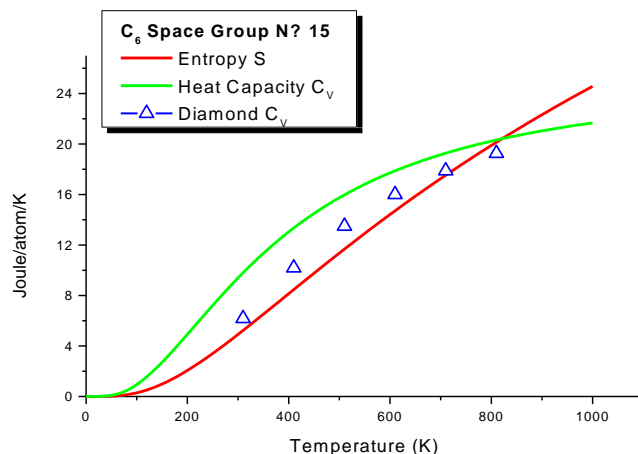


Figure 5. Entropy and specific heat at constant volume of tetragonal tet- C_6 as functions of temperature. Experimental C_v data for diamond are shown as blue triangles

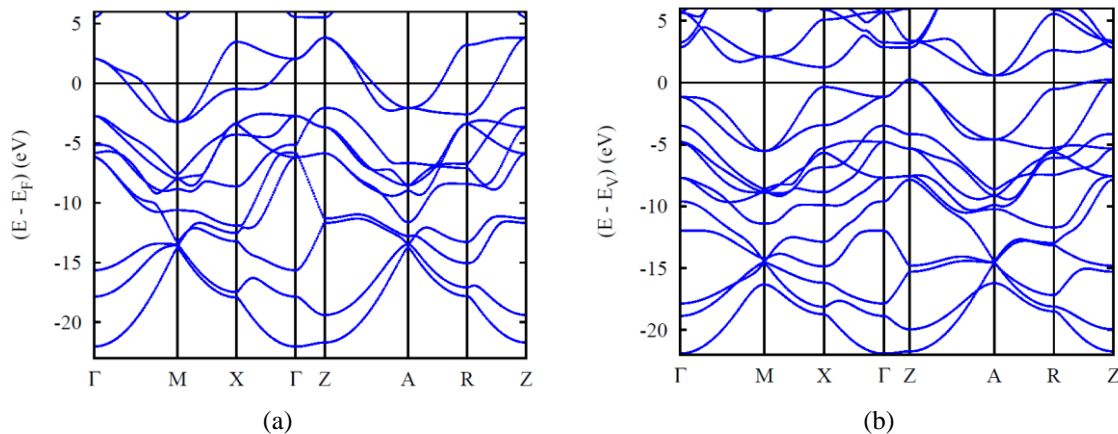


Figure 5. Electronic band structures of a) C_5 , b) C_6

3.4 Electronic band structures

Using the crystal parameters in Table 1, the electronic band structures shown in Figure 4 were obtained using the all-electrons DFT-based augmented spherical method (ASW) [21] and the same gradient GGA XC functional [13]. The bands develop along the main directions of the primitive tetragonal Brillouin zone. We focus on the electronic properties of C_5 and C_6 having close structural and mechanical properties. C_5 (Fig. 5a) is found with metallic-like character with bands crossing the Fermi level E_F . Oppositely C_6 (Fig. 5b) is identified as small gap semiconductor with the top of the valence band dominated by delocalized π electrons, and the zero-energy is with respect to the top of the valence band E_V .

4. Conclusions

Novel tetragonal C₆ is a semi-conducting original carbon allotrope characteristic of mixed sp²/sp³ carbon hybridizations. Characterized as mechanically and dynamically stable, C₆ can be considered as a hard anisotropic material with phonon band structure featuring allene-like tricarbon (sp²) embedded in tetrahedral lattice of C(sp³).

Such original hybrid sp²/sp³ electronic configurations found in nanodiamonds, induce a growing interest in materials investigations as electrochemical ones recently exposed by Zhai et al. [31], and novel C₆ is illustrative of such behavior within the simplest cell possessing equal amounts of three C(sp²) and three C(sp³). Prospective works aiming at reducing the amount of C(sp²) within diamond are underway.

Acknowledgments

I am grateful to Dr. Vladimir Solozhenko Directeur de Recherche at CNRS-Paris for exchanges and expertise in hard materials.

Conflict of interest

There is no conflict of interest for this study.

References

- 1 Oganov, A.R. (2018). Crystal structure prediction: reflections on present status and challenges. *Faraday Discuss.* 211, 643.
- 2 Hoffmann, R.A, Kabanov, A, Goloy, A.A., & Proserpio, D. M. (2016). *Homo Citans* and Carbon Allotropes: For an Ethics of Citation . *Angew. Chem. Int. Ed.*, 2016, 55, 10962–10976. and SACADA database (*Samara Carbon Allotrope Database*). www.sacada.info
- 3 Matar, S.F.(2022). CCDC 2208344: (Refcode NEQHUQ; name C6POLr), DOI:[10.5517/ccdc.csd.cc2d3yxd](https://doi.org/10.5517/ccdc.csd.cc2d3yxd)
- 4 Matar, S.F. & Solozhenko, V.L. (2022). The simplest dense carbon allotrope: Ultra-hard body centered tetragonal C₄. *J. Solid State Chem.* 314, 123424 & Corrigendum to “The simplest dense carbon allotrope: Ultra-hard body-centered tetragonal C₄” <https://doi.org/10.1016/j.jssc.2022.123587>
- 5 Liu, Chao & Lingyu, Liu & Ying, Pan. (2022). Stability, deformation, physical properties of novel hard B2CO phases. *Journal of Materials Science.* 57. 10.1007/s10853-022-07242-4.
- 6 Hohenberg, P. & Kohn, W (1964). Inhomogeneous electron gas. *Phys. Rev. B* 136, 864-871.
- 7 Kohn, W. & Sham, L.J. (1965). Self-consistent equations including exchange and correlation effects. *Phys. Rev. A* 140, 1133-1138.
- 8 Matar, S.F. (2023). Novel Ultrahard Carbon Allotrope C₅ with Mixed sp²/sp³ Carbon Hybridizations. Crystal chemistry and First Principles Investigations. *Acta Scientifc Applied Physics* 3.1: 02-09. <https://arxiv.org/abs/2210.04210>
- 9 Bullett, D. W (1982). Structure and bonding in crystalline boron and B₁₂C₃. *Journal of Physics C: Solid State Physics*, 15, 415.
- 10 Matar, S.F, Etourneau, J, & Solozhenko V.L (2022). First-principles investigations of tricarbon: From the isolated C₃ molecule to a novel ultra-hard anisotropic solid. *Carbon Trends.* 6, 100132.
- 11 Kresse, G. & Joubert, J (1994). From ultrasoft pseudopotentials to the projector augmented wave. *Phys. Rev. B* 59 1758-1775.
- 12 P.E. Blöchl, Projector augmented wave method. *Phys. Rev. B* 50 17953-17979.
- 13 Perdew, J., Burke, K. & Ernzerhof, M (1996). The Generalized Gradient Approximation made simple. *Phys. Rev. Lett.* 77 3865-3868.
- 14 W.H. Press, B.P. Flannery, S.A. Teukolsky, W.T. Vetterling, *Numerical Recipes*, 2nd ed., Cambridge University Press: New York, USA, 1986.
- 15 P.E. Blöchl, O. Jepsen, O.K. Anderson, Improved tetrahedron method for Brillouin-zone integrations. *Phys. Rev. B* 49 (1994) 16223-16233.
- 16 M. Methfessel, A.T. Paxton, High-precision sampling for Brillouin-zone integration in metals. *Phys. Rev. B* 40 (1989) 3616-3621.
- 17 H.J. Monkhorst, J.D. Pack, Special k-points for Brillouin Zone integration. *Phys. Rev. B* 13 (1976) 5188-5192.
- 18 Voigt, W. (1889). Über die Beziehung zwischen den beiden Elasticitätsconstanten isotroper Körper. *Annal. Phys.* 274, 573-587.

- 19 Togo, A. & Tanaka, I. (2015). First principles phonon calculations in materials science”, *Scr. Mater.*, 108, 1-5.
- 20 Momma, K. & Izumi, F (2011). VESTA 3 for three-dimensional visualization of crystal, volumetric and morphology data. *J. Appl. Crystallogr.*, 44, 1272-1276.
- 21 Eyert, V (2000). Basic notions and applications of the augmented spherical wave method. *Int. J. Quantum Chem.* 77, 1007-1031
- 22 Wallace, D.C. Thermodynamics of crystals. New York, USA: John Wiley and Sons; 1972.
- 23 Brazhkin, V. & Solozhenko, V. L (2019). Myths about new ultrahard phases: Why materials that are significantly superior to diamond in elastic moduli and hardness are impossible. *J. Appl. Phys.* 125, 130901 <https://doi.org/10.1063/1.5082739>.
- 24 F. Birch, J. Geophys. Res. 83 (1978) 1257
- 25 Lyakhov, A.O. & Oganov, A.R (2011). Evolutionary search for superhard materials: Methodology and applications to forms of carbon and TiO₂. *Phys. Rev. B* 84, 092103.
- 26 Mazhnik, E. & Oganov, A.R. (2019). A model of hardness and fracture toughness of solids. *J. Appl. Phys.* 126 125109.
- 27 Krishnan, R.S (1945). Raman spectrum of diamond. *Nature* 155, 171.
- 28 Dove M.T., Introduction to Lattice Dynamics, Cambridge University Press, 1993.
- 29 Victor A.C. (1962), Heat capacity of diamond at high temperatures, *J. Chem. Phys.* 36 1903–1911
- 30 Chenhan Liu, Yunfei Chen, and Chris Dames (2019). Electric-Field-Controlled Thermal Switch in Ferroelectric Materials Using First-Principles Calculations and Domain-Wall Engineering. *Phys. Rev. Applied* 11, 044002
- 31 Zhai, Z. Huang, N. & Jiang, X (2022). Progress in electrochemistry of hybrid diamond/sp²-C nanostructures. *Current Opinion in Electrochemistry*, 32, 100884. <https://doi.org/10.1016/j.coelec.2021.100884>